Low temperature water–gas shift: role of pretreatment on formation of surface carbonates and formates

Gary Jacobs*, Patricia M. Patterson, Leann Williams, Dennis Sparks, and Burtron H. Davis

University of Kentucky, Center for Applied Energy Research, 2540 Research Park Drive, Lexington, KY 40511

Received 30 January 2004; accepted 27 April 2004

Recently, the role of ceria vacancies on water–gas shift activity has been explained in terms of a redox mechanism, whereby CO adsorbed on a metal reduces the ceria surface to generate CO_2, and water reoxidizes the ceria surface to CeO_2, liberating hydrogen in the process. In this study, we examine the possibility of a ceria-mediated redox mechanism by examining more closely the evolution of carbonate and formate bands under different controlled treatment environments, and utilizing different reduction procedures. Earlier it was claimed that the decomposition of carbonates by water was consistent with a redox process, whereby the CO_2 product could spillover to the support. We found that the observation of carbonate formation and decomposition by water was a result of the treatment procedure used in the earlier work, and that, once bridging OH groups are produced in the presence of water, the reaction more likely proceeds via a formate intermediate, which is produced by reaction of CO with the active bridging OH groups. However, the vacancies appear to play an important role in generating these active sites. Possible pathways to active site generation are discussed.

KEY WORDS: water–gas shift; vacancies; low-temperature shift (LTS); ceria; platinum; kinetic isotope effect; DRIFTS.

1. Introduction

Proton exchange membrane fuel cells (PEMFC) fueled with hydrogen may replace the internal combustion engine in the future. However, before any benefit can be realized from the PEMFC, hydrogen of sufficient purity must be generated [1–3]. CO is especially problematic, as parts per million levels poison the noble metal catalysts used in the fuel cell. The product stream from reforming contains about 8–10% CO, and these levels are reduced to about 3–5% by high temperature water–gas shift (HTS) catalysts that operate at or close to equilibrium [4]. Low temperature shift (LTS) can be used after HTS to achieve higher CO conversions, but effective catalysts must be designed so that, in conjunction with preferential oxidation (PROX) to convert CO to CO_2, levels below 5 ppm can be achieved. In this way, the implementation of costly H_2-permeable membranes may be avoided.

One catalyst system receiving considerable attention for LTS is ceria loaded with metal promoters, such as platinum. It is anticipated that, with proper development, metal promoted ceria catalysts should realize much higher CO conversions than even commercial CuZnO catalysts.

There is still an ongoing debate regarding the roles played by ceria and the metal as promoters for water–gas shift (WGS). However, there are primarily two popular mechanisms. One mechanism is a redox process involving reaction of adsorbed CO with ceria at the metal–support interface to produce CO_2, with the replenishing of the surface oxygen vacancy with the oxygen from water to generate H_2 [5–8]. Another mechanism was proposed to proceed via surface formates [9,10]. In that scheme, reaction of CO with ceria hydroxyl groups generates surface formates, the proposed intermediate for the reaction. The active bridging OH groups occur on a reduced ceria surface, (i.e., core remains Ce^{+4}) whereby surface oxygen atoms have been removed and/or converted to OH. This mechanism has been used not only to describe the catalysis on ceria [9–11], but for other systems as well, including ZnO [12] and MgO [13] for WGS and Cr_2O_3 [14] for methanol decomposition.

In preliminary studies where a high H_2O/CO ratio was employed, Pt/ceria catalysts were examined by IR spectroscopy [15,16]. It was found that not only did addition of CO to partially reduced ceria generate significant bands characteristic of surface formates, the surface formate coverages were controlled by the WGS rate under steady-state reaction conditions. In contrast, the Pt–CO band displayed very little change under these reaction conditions. We compared our findings to the rate law for metal promoted ceria catalysts obtained from kinetic studies [7]:

$$\text{Rate} = k_1 k_2 P_{CO} P_{H_2O} / (k_1 P_{CO} + k_2 P_{H_2O})$$

According to the rate expression, CO exhibits a first order partial pressure dependency at high H_2O/CO ratios, and therefore, the adsorbed CO intermediate for

*To whom correspondence should be addressed.

1011-372X/04/0700–0097/0 © 2004 Plenum Publishing Corporation

WGS should move to lower surface coverages with increasing reaction rate. Therefore, according to our previous results, only the surface formate mechanism satisfied the kinetic criteria.

In a separate investigation, XANES results [17] indicated that although Pt did assist in catalyzing reduction of the surface shell of ceria, the partially reduced ceria did not reoxidize when considerable amounts of water were introduced into the hydrogen feed. Such reoxidation would be necessary to substantiate a ceria-mediated redox process under the hydrogen-containing atmosphere found in a fuel processor.

The use of isotope switching (H_2O to D_2O) in combination with IR spectroscopy was also employed to gain insight into the reaction mechanism of LTS [9,18–20]. The easily observed kinetic isotope effect strongly suggests that C–H bond breakage is linked to the rate limiting step of the reaction. Not only did the CO conversion decrease when H_2O was switched to D_2O, but the surface coverage of H-formate was much lower during WGS than D-formate, indicating that the H-formate reacts faster than D-formate, consistent with the change in CO conversion. We attributed the rate limiting step to the decomposition of surface formates, as was proposed earlier by Shido and Iwasawa [9,10].

In an earlier study, hydrogen reduction was utilized as the pretreatment. This pretreatment was criticized on the basis that the formates may be the result of a contaminated sample following activation. It was recommended that oxygen be utilized as a pretreatment prior to a CO reduction. In this study, various activation procedures have been employed and their impact on surface formate and carbonate species has been defined.

2. Experimental

2.1. Catalyst preparation

High surface area ceria was prepared *via* homogeneous precipitation from a nitrate solution with urea and aqueous ammonia in a manner similar to Li *et al.* [7]. The preparation was an adaptation of work conducted on $CuO–ZrO_2$ methanol synthesis catalysts [21], whereby urea decomposition is a slow process resulting in a slower, more homogeneous approach to precipitation. On a basis of 30 g CeO_2, an appropriate amount of $Ce(NO_3)_3{\cdot}6H_2O$ (Alfa Aesar, 99.5%) and 240 g urea (Alfa Aesar, 99.5%) were dissolved in 900 mL of deionized water, and to the solution about 30 ml NH_4OH (Alfa Aesar, 28–30% NH_3) was added dropwise (~1 mL/min). The mixture was then boiled at 100 °C with constant stirring. The precipitate was filtered, washed with 600 ml of boiling deionized water, and dried in an oven (100 °C) overnight. The dried precipitate was then crushed and calcined in air in a muffle furnace at 400 °C for 4 h.

2.2. Brunner Emmet Teller (BET) surface area

BET surface area measurements were carried out in a Micromeritics Tristar 3000 gas adsorption analyzer. For each sample a weight of approximately 0.25 g was used. The adsorptive gas was nitrogen (N_2) and the adsorption was carried out at the boiling temperature of liquid nitrogen.

2.3. Temperature programmed reduction (TPR)

TPR was conducted on CeO_2 supports and metal promoted catalysts in a Zeton-Altamira AMI-200 unit, which was equipped with a thermal conductivity detector (TCD). Argon was used as the reference gas, and 10% H_2 (balance Ar) was flowed through the sample at 30 ccm as the temperature was increased from 50 to 800 °C at a ramp rate of 10 °C/min. A liquid nitrogen trap was used to capture any water that evolved from the catalyst prior to the gas entering the TCD.

2.4. Diffuse reflectance infrared fourier transform spectroscopy (DRIFTS)

A Nicolet Nexus 870 was used, equipped with a DTGS-TEC detector. A high pressure/high temperature chamber fitted with ZnSe windows was utilized as the WGS reactor for *in situ* reaction measurements. The gas lines leading to and from the reactor were heat traced, insulated with ceramic fiber tape, and further covered with general purpose insulating wrap. Scans were taken at a resolution of 4 to give a data spacing of 1.928 cm^{-1}. Typically, 128 scans were taken to improve the signal-to-noise ratio. The sample amount was 33 mg of powder.

A steam generator consisted of a downflow tube packed with quartz beads and quartz wool heated by a ceramic oven and equipped with an internal thermocouple. The lines after the steam addition were heat traced. The steam generator and lines were run at the same temperature as that at the *in situ* sample holder of the DRIFTS cell. This allowed us to accurately bring the reactants to the desired reaction temperature. Water was added to the steam generator through a thin needle welded to a 0.16 cm line. Two precision ISCO Model 500D syringe pumps were used to feed the water or deuterated water, and the system was equipped with a selector valve.

Feed gases were controlled using Brooks 5850 series E mass flow controllers. Iron carbonyl traps consisting of lead oxide on alumina (Calsicat) were placed on the CO gas line. All gas lines were filtered with Supelco O_2/moisture traps.

3. Results and discussion

3.1. Standard characterization

Standard characterization procedures were reported in our earlier work [15–20]. Briefly, the ceria has a BET surface area of 105 m^2/g. Using XRD and integral breadth analysis for the peak at 28.8 ° corresponding to the (111) plane indicated that the domain size of the ceria was approximately 8.4 nm.

The TPR profiles in figure 1 show two important features. By comparing the reduction profiles of sintered ceria and HSAUP ceria, the bulk ceria is assigned to reduction at close to 750 °C. Reduction of the surface shell of ceria, present as a large broad peak on the high surface area ceria, occurs between 400 and 500 °C. Pt catalyzes and therefore shifts the peak for the reduction of the surface shell of ceria to lower temperatures, but has little effect on the bulk reduction. The catalysis causing the shift of the surface reduction to lower temperature was confirmed by pulse reoxidation measurements after reduction at 300 °C and by *in situ* XANES studies on both unpromoted and metal promoted catalysts. They are not reproduced in this work but are described in [17–19].

3.2. In situ *DRIFTS studies*

In a recent communication to us, it was commented that the formates we observed may arise due to sample contamination. Therefore, it was recommended that we first carry out an *in situ* O_2 calcination prior to a CO reduction (whereas before, we used hydrogen). However, such a procedure may circumvent the generation of bridging OH groups on the catalyst surface. In previous IR studies, we typically carried out a hydrogen reduction on the catalyst which produced OH groups and/or the water generated during the reduction reacted with oxygen vacancies to produce bridging OH groups on the surface of partially reduced ceria.

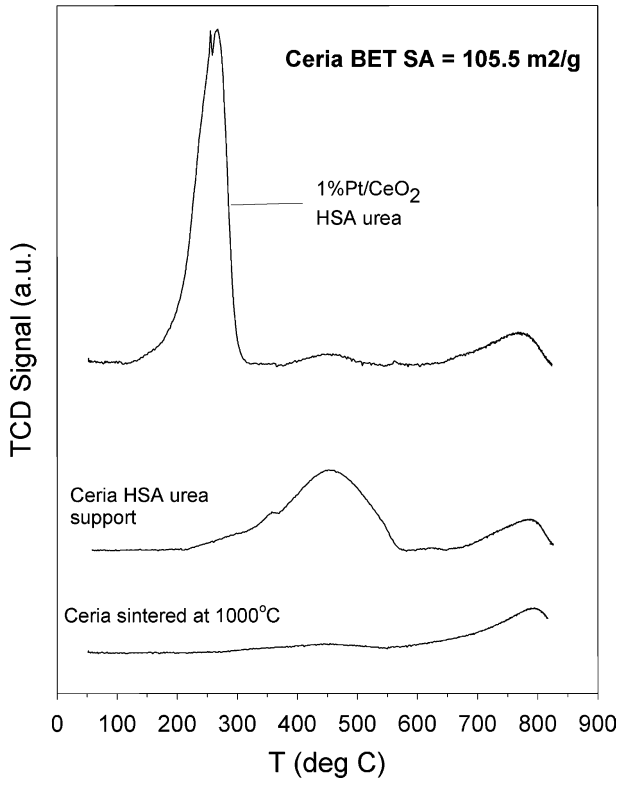

Figure 1. TPR profiles for, moving upward, unpromoted ceria sintered at 1000 °C, unpromoted ceria HSA urea method, and 1%Pt promoted HSA urea method ceria.

Dissociation of water to produce the bridging OH groups requires that the oxidation state of ceria does not change. For consistency we continue to use the terminology of bridging or geminal OH groups although direct evidence for these structures is weak, at best. The usage of bridging OH groups is based primarily on assignments made by Montagne *et al.* [22] and Laachir [23]. However, these assignments were based solely on vibrational frequencies and not by comparison with reference compounds containing geminal OH species. We have not observed a change of oxidation state to partially reduced ceria in switching from H_2:He to H_2:He:H_2O in XANES experiments [17,18].

The overall reduction of ceria can be written as

$$2CeO_2 + H_2 \rightarrow Ce_2O_3 + H_2O \qquad (1)$$

In the reaction in equation (1), all cerium ions are reduced from the 4+ to the 3+ valence state. However, reduction at the lower temperatures used in this study is limited to essentially those cerium ions located in the surface layer; the bulk cerium ions are not reduced at low temperature, as suggested by equation (1). For surface reduction with the desorption of water the reaction for the partial reduction (reduction of the surface and not the bulk) can be represented schematically as

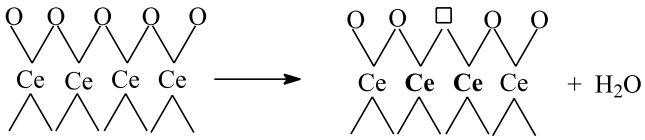

(2)

where □ represents an anion vacancy (i.e., absence of O^{2-}) and the bold Ce represents Ce^{3+} rather than Ce^{4+}. However, equation (2) does not represent the experimental observation where hydroxyl groups are identified in the IR spectrum. Based upon past assignments of the wavelength of the OH absorption, this band has been assigned to bridging OH groups which can be represented by the chemical structure O–$Ce^{3+}(OH)_2$. The assignment of this band as representative of bridging OHs was by analogy with thoria, and here the assignment was made based on the assumption that the bridging OH band would fall between those of MOH and $M(OH)_3$. The experimental evidence from IR indicates that some or all of the hydrogen reacts to produce OH groups. Two ways that the OH groups could be formed during reaction with hydrogen are illustrated schematically below:

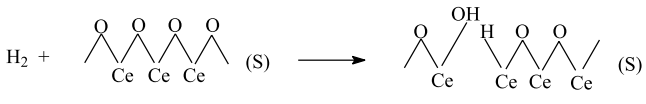

(3)

The chemistry in equation (3) is analogous to the reduction of ZnO where numerous authors (e.g., [24] and [25–28]) have shown that hydrogen dissociates heterolytically to produce H^+ and H^- which react to produce −ZnOH and ZnH. Unfortunately, the band expected for CeH falls in the region where strong OCO bands of residual carbonates are located. CeD is expected, by analogy to the position of the ZnD band, to fall at a lower frequency than CeH, and where it should not be obscured by the OCO bands; however, a band for CeD was not observed following reaction of CeO_2 with D_2. The failure to observe a band that could be assigned to CeD does not permit us to conclusively eliminate the possibility of reaction (3) which would be consistent with observation of the storage of H (or D) during the reaction of ceria with hydrogen (or deuterium).

Hydrogen can also effect reduction of Ce^{4+} through heterolytic dissociation with the simultaneous reduction of Ce^{4+} to Ce^{3+} and the formation of bridge bonded OH groups:

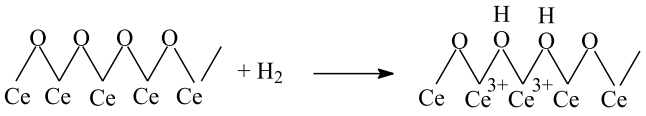

(4)

This reaction can continue until all of the surface Ce^{4+} ions are reduced to Ce^{3+} and all surface O^{2-} ions are converted to bridge bonded OH groups. This produces, in effect, Ce^{3+} ions that contain bridging OH groups. This idealized system would allow the adsorption of one H for each surface Ce ion, as observed by Johnson and Mooi [29]. This idealized structure could explain the observation of two IR bands for the pseudo-geminal OH groups.

The bridging OH structure may help in explaining the presence of a shoulder in the high wave number portion of the geminal OH band in IR spectroscopy, as one can define two possible vibrational modes for Ce–O–Ce bonding – asymmetric and symmetric, which could in turn influence the O—H stretch.

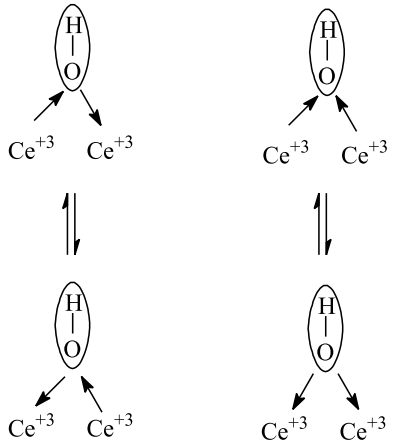

The utility of ceria to store and release oxygen in auto catalysts has led to a vast literature on ceria. While much of the work is with supported ceria catalysts, considerable work has been done with pure ceria and with noble metals supported on ceria (e.g., [30,31]). A direct relationship has been observed between the surface area of ceria and the amount of hydrogen consumed during the reduction [29]. This has been interpreted to show that the lower temperature reduction is restricted to the surface oxygen and has been reproduced by several groups. What happens during and following reaction with hydrogen has not been defined. Hydrogen is considered to interact with ceria in two ways: reversibly, with uptake of hydrogen, and irreversibly, with loss of water [32]. It has been reported that only molecularly adsorbed water and CO were observed on oxidized ceria or Rh-ceria [33]. The reduced Rh-ceria surface was more reactive and promoted the dissociation of both water and CO, with CO preferentially adsorbing on Rh and water on ceria. On reduced ceria and Rh-ceria, chemisorbed water and hydroxyls are produced. On Rh-free ceria, chemisorbed water desorbs below 27 °C and hydroxyls decompose above 227 °C to give hydrogen as a product. Rh promotes the dissociation of chemisorbed water and the production of hydrogen in the range from −73 to 27 °C; Rh also promotes the dissociation of hydroxyls to produce hydrogen. A number of recent papers have indicated that reduced ceria can be easily re-oxidized by water but these conclusions appear to be based primarily on the work of Otsuka *et al.* [34] which was done in a recirculation reactor at low partial pressures of water. Hydrogen recovery by the reaction with water at 400°C was not equal to the hydrogen consumed in the reduction step at 600 °C. However, they reported that some metal promoted ceria catalysts showed greater than 50% reoxidation by water in less than two minutes for reaction at 200 °C. Fallah *et al.* [35] indicate that between 300 and 400 °C the reduction starts on the surface through successive hydrogen dissociation and anionic vacancy formation, followed by a much slower bulk diffusion step. These authors obtained a weight loss and attribute this to the formation and desorption of water. In contrast, graviometric [23,36] and TPD [37] results indicate that water elimination does not occur below 252 °C. In agreement with other authors, Fallah *et al.* [35] found that the presence of a noble metal caused the reduction rate to be increased and the rate of reoxidation to be retarded. The results indicated that the high surface area caused the surface process to dominate the bulk process, effectively eliminating significant bronze (CeO_2H_x) formation. Fallah *et al.* [35] provided a mechanism that is described by equation (1).

On the other hand, the failure of water to re-oxidize ceria has been noted. Sadi *et al.* [38] determined the oxidation by water of samples that had been reduced in the 300–900 °C range and found that samples reduced at or below 500 °C were not, or only slightly, re-oxidized at

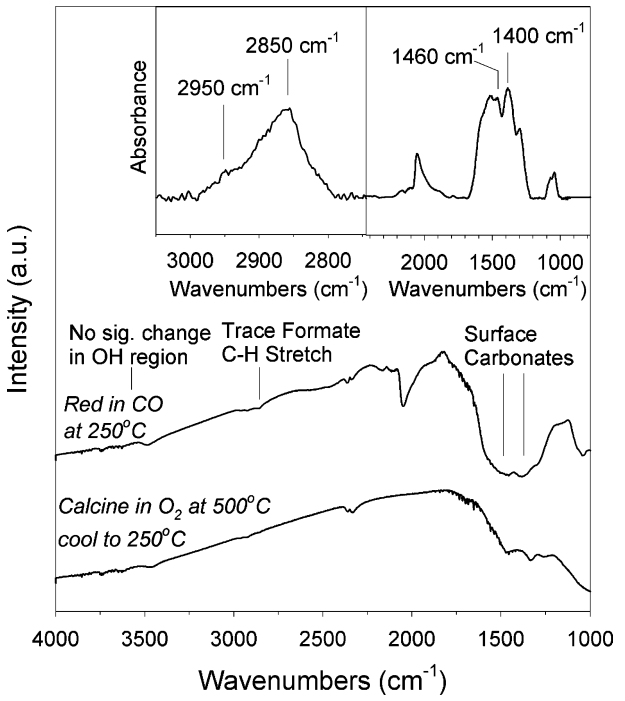

Figure 2. 1%Pt/ceria after calcination in O_2 (100 ccm) at 500 °C and after reduction in CO (3.75 ccm: 135 ccm N_2) at 250 °C. (Insert) Difference spectra for OCO and CH regions in absorbance to highlight changes observed.

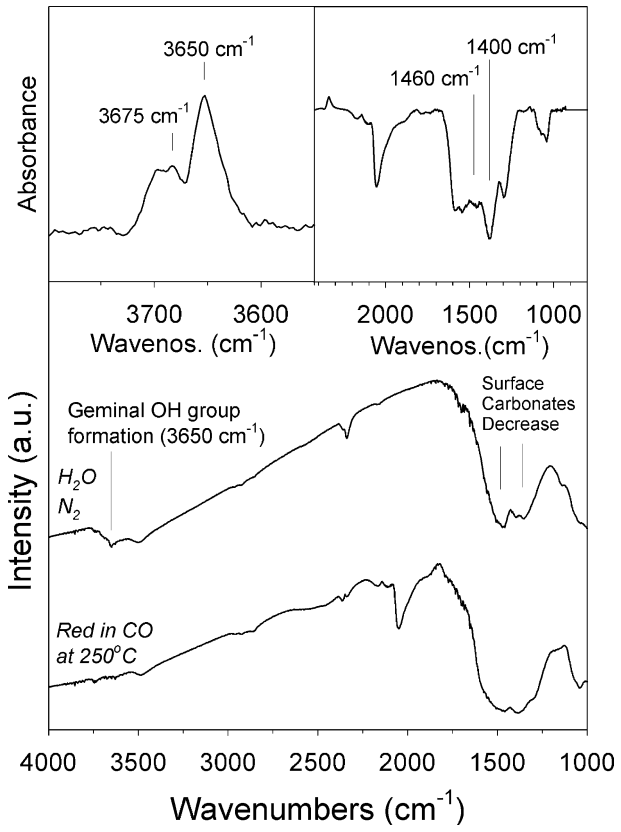

Figure 3. 1%Pt/ceria after reduction in CO (3.75 ccm: 135 ccm N_2) at 250 °C and after purging in N_2 (200 ccm) and adding water (125 ccm: 10 ccm N_2). (Insert) Difference spectra for OCO and OH regions in absorbance to highlight changes observed. $T = 250$ °C.

500 °C by water. In contrast, when the sample was reduced at 850 °C, re-oxidation by water was complete even at room temperature. Using deuterium tracers, the authors showed that deuterium was stored so that it did not mix with hydrogen present in the added water and that essentially pure H_2 was evolved. They propose that the reaction of steam with reduced ceria may be used as an analytical approach to determine the number of reduced centers.

Reduction with CO at higher temperatures can be visualized as

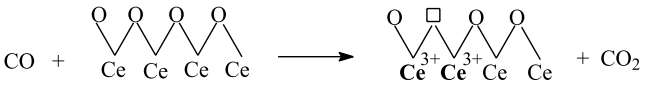

(5)

Thus, reaction with CO of a catalyst calcined in O_2 at 500 °C to produce a surface that is expected for stoichiometric CeO_2 should follow the above reduction, and circumvent formation of bridging OH groups. The spectra shown in figure 2 confirm this expectation. However, instead of a defect surface, the spectrum shows that surface carbonates are formed, as observed by Hilaire *et al.* [6], and the similarity between our spectra and their work is striking (carbonate OCO bands at ca. 1400 and 1460 cm^{-1}). No C–H stretching bands (ca. 2850 and 2945 cm^{-1}) are observed in figure 2 to indicate the OCO vibrations correspond to surface formates. As shown in figure 3, the addition of water to this sample removes a considerable fraction of the carbonate bands.

It is strongly stressed, however, that this does not provide evidence for a ceria-mediated redox process. In fact, to assume such a mechanism takes place is to neglect the presence of water in the reformer. The data in Figure 3 show only that some surface carbonate is removed when the bridging OH groups are formed by the addition of water. Thus, reduction with CO and then reaction with water may be interpreted by equation (6):

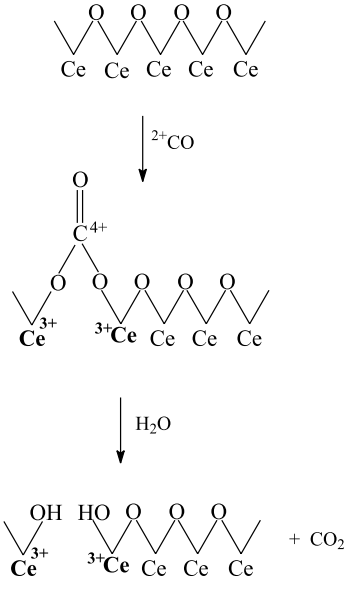

(6)

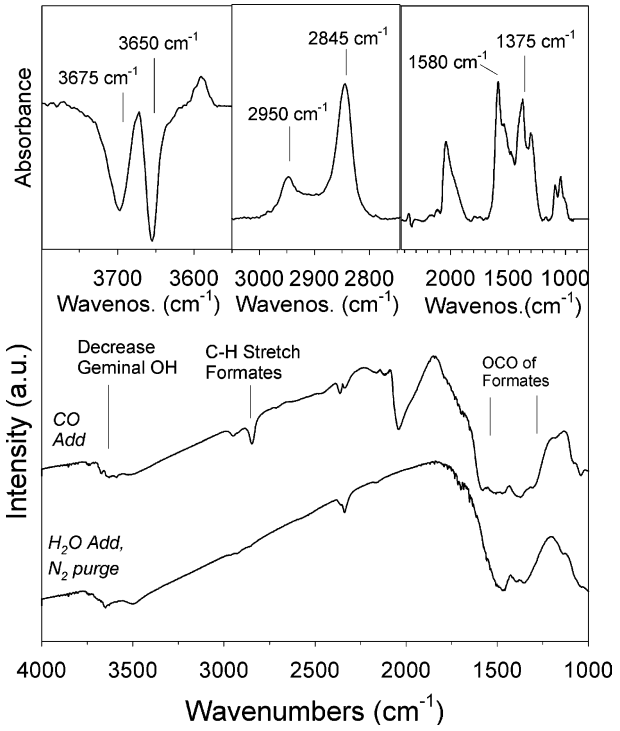

Figure 4. 1%Pt/ceria after adding water (125 ccm: 10 ccm N_2) to activate geminal OH groups, then purging in N_2 (200 ccm), and after adsorbing CO (3.75 ccm: 135 ccm N_2) to react with the geminal OH groups to generate formates. (Insert) Difference spectra for OCO, CH, and OH regions in absorbance to highlight changes observed. $T = 250$ °C.

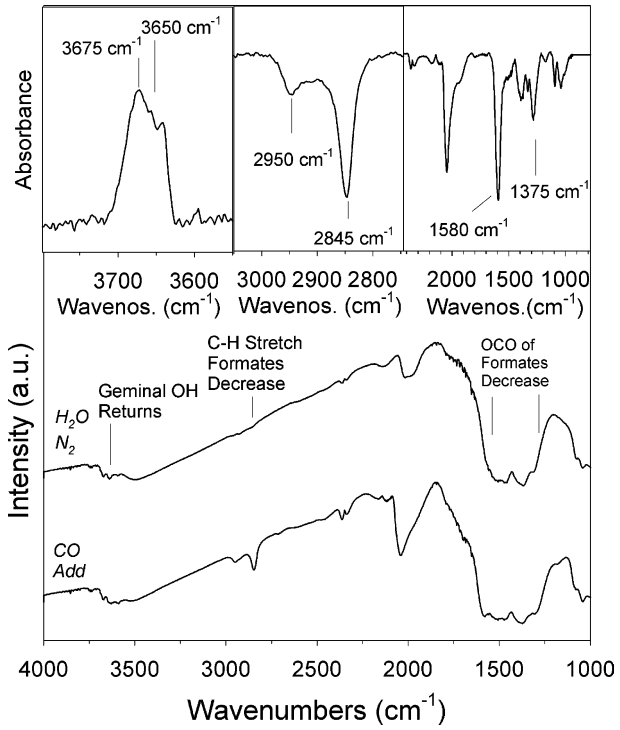

Figure 5. 1%Pt/ceria after adsorbing CO (3.75 ccm: 135 ccm N_2) to react with the geminal OH groups to generate formates, and after adding water (125 ccm: 10 ccm N_2) to decompose the formates and purging in N_2 (200 ccm) to give back the geminal OH groups. (Insert) Difference spectra for OCO, CH, and OH regions in absorbance to highlight changes observed. $T = 250$ °C.

The data in figure 3 clearly show that bridging OH groups are formed following the addition of water, as indicated by the band at approximately 3650 cm^{-1} (see absorbance spectra at top) after water addition, and recorded after the gas phase water is purged with inert N_2 gas.

The following describes a critical test for discriminating between the formate and redox mechanisms. Bridging OH bands have been proposed to be the active site by different groups [9,10,15–20]. If this is the case, adsorption of CO should lead to a reaction with these groups to produce surface formates. The spectra in figure 4 show that formates are indeed formed after addition of CO. They are marked by the OCO asymmetric and the symmetric stretching vibrations at 1580 and 1375 cm^{-1}, and these bands are accompanied by CH stretching vibrations at 2850 and 2945 cm^{-1}. Also, the bands at ca. 3650 cm^{-1}, corresponding to bridging OH groups, decrease when CO is adsorbed.

Not surprisingly, the formates decompose readily to produce CO_2 and H_2 once water is introduced. As we have noted in other reports [15,17], the decrease of the formate bands is more rapid with time than the decrease of the Pt–CO band, suggesting that they are the important intermediates for the WGS reaction. Also, as discussed earlier, under steady state conditions when a high H_2O/CO ratio is used, the surface formate concentrations are controlled by the WGS rate (i.e., become lower intensity with higher rate in comparison with the saturated site condition), while Pt–CO remains saturated at high H_2O/CO ratios, where the WGS reaction is first order in CO. The data shown in figures 5–7 are provided to detail these features. Addition of CO to the bridging OH bands causes formates to form, and these are decreased with water addition. After the bridging OH groups are produced, the carbonates do not change, but remain on the surface. Virtually only the surface formates undergo reaction, whereas carbonates decompose very slowly with time.

Figure 8 shows the sensitivity of treatment and reduction procedure on the direct production of surface formates. If hydrogen is used, starting from room temperature, and then CO is added, strong formate bands are produced. This is because hydrogen reacts to produce OH and/or water, if produced from the reduction, reacts with vacancies to generate the bridging OH groups during the reduction step. Moving upward in figure 8, calcining at 400 °C in air and using CO still produces formates directly, but also carbonates along with them. This is a result of the presence of a combination of vacancies and

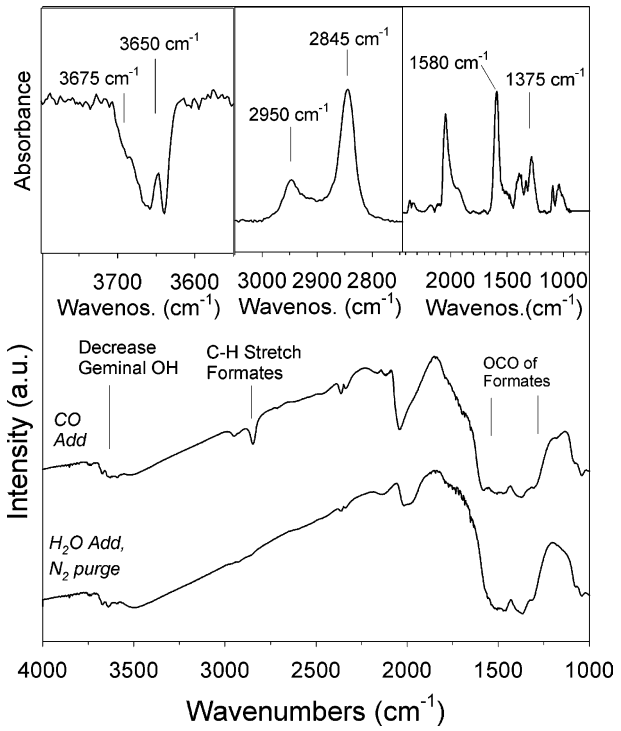

Figure 6. 1%Pt/ceria after adding water (125 ccm: 10 ccm N_2) to regenerate geminal OH groups, then purging in N_2 (200 ccm), and after adsorbing CO (3.75 ccm: 135 ccm N_2) to react with the geminal OH groups to generate formates again. (Insert) Difference spectra for OCO, CH, and OH regions in absorbance to highlight changes observed. $T = 250$ °C.

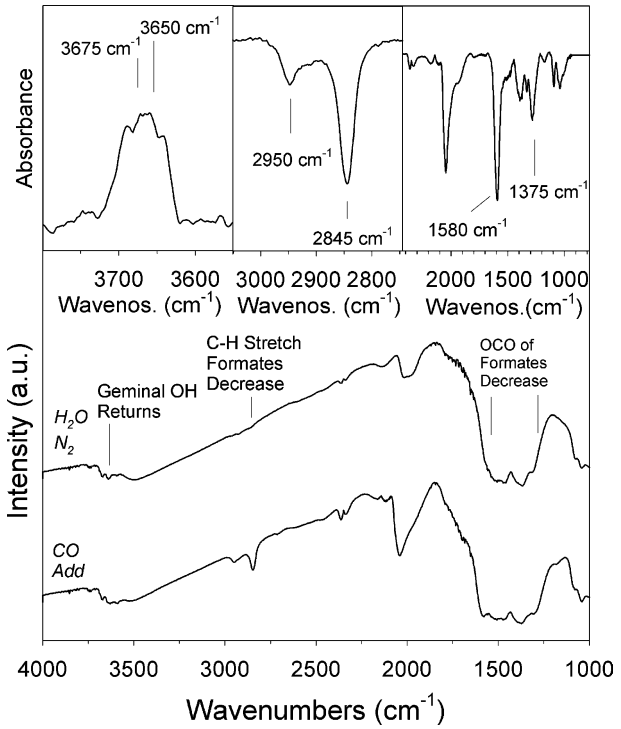

Figure 7. 1%Pt/ceria after adsorbing CO (3.75 ccm: 135 ccm N_2) to react with the geminal OH groups to generate formates, and after adding water (125 ccm: 10 ccm N_2) to decompose the formates and purging in N_2 (200 ccm) to give back the geminal OH groups. (Insert) Difference spectra for OCO, CH, and OH regions in absorbance to highlight changes observed. $T = 250$ °C.

bridging OH groups on the surface. Therefore, to facilitate the observation of formate intermediates, the carbonates need to be removed, or significantly decreased, by a water addition step, as observed previously. Finally, calcining with O_2 at 500 °C and reducing the catalyst with CO circumvents the direct generation of the bridging OH groups. Thus, only carbonates are observed after the CO reduction step. To obtain the bridging OH groups, the carbonates need to be removed by water addition. It appears that some researchers have mistakenly taken this removal of carbonates when water is added as evidence for a redox mechanism. Carbonates are removed and bridging OH groups are formed when water is added. Subsequent CO addition and water removal steps clearly show that a formate mechanism is likely operating for LTS.

The formate mechanism for the WGS reaction catalyzed by partially reduced ceria may be viewed as:

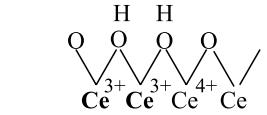

(7a)

CO

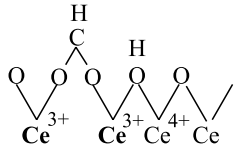

(7b)

H_2O

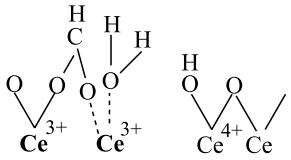

(7c)

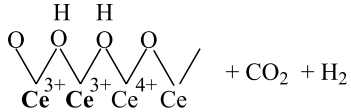

(7d)

The decomposition of the adsorbed formate (7b) to produce CO_2 is unlikely since this would lead to a hydride ion [H^-] bridging two Ce^{+3} ions. However, adsorption of water on one of the Ce^{3+} ions allows this to occur by forming H_2 as the CO_2 is expelled. Since the formate CH (or C–D) bond is broken during the decomposition, a normal kinetic isotope effect is expected, as we and others have confirmed. The absence

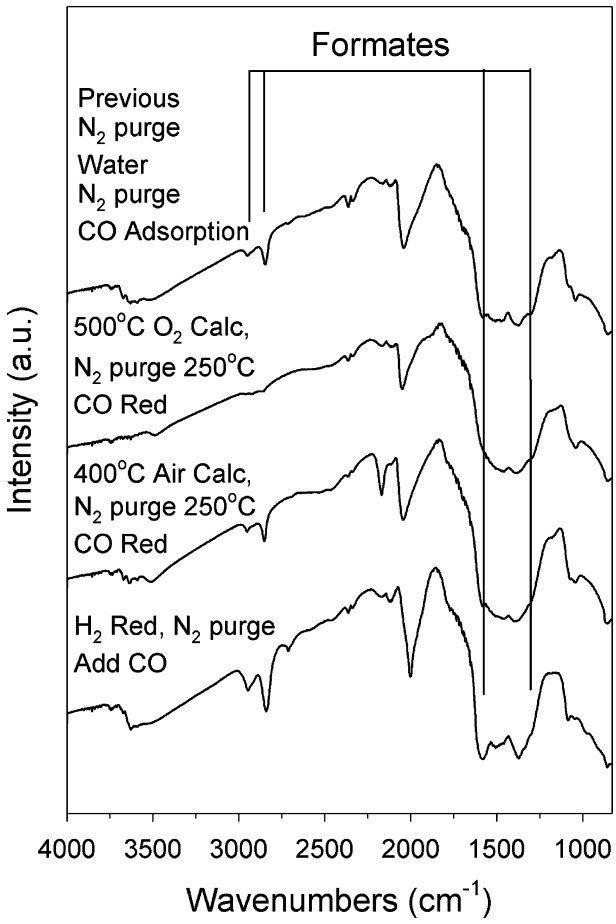

Figure 8. Impact of treatment and reduction procedures on the direct production of formates. Moving upwards: (1) H_2 reduction at 250 °C (100 ccm: 135 ccm N_2), N_2 purge (135 ccm N_2), CO addition (3.75 ccm CO: 135 ccm N_2) at 250 °C; (2) Air calcination at 400 °C (100 ccm air), N_2 purge (135 ccm N_2), CO reduction (3.75 ccm CO: 135 ccm N_2) at 250 °C; (3) O_2 calcination at 400 °C (100 ccm air), N_2 purge (135 ccm N_2), CO reduction (3.75 ccm CO: 135 ccm N_2) at 250 °C; (4) N_2 purge (135 ccm N_2), H_2O (125 ccm: 10 ccm N_2), N_2 purge (135 ccm N_2), and CO adsorption (3.75 ccm CO: 135 ccm N_2) at 250 °C.

of a kinetic isotope effect when HCO_2^- reacts with D_2O (or DCO_2^- reacts with H_2O) suggests that the formate decomposition may be viewed as

$$OH^- + CO^- \rightarrow H\ CO_{2^-}$$

$$HCO_2^- \rightarrow CO_2 + H^- \qquad (8)$$

$$D_2O + H^- \rightarrow HD + OD^-$$

4. Conclusions

Treatment conditions and the reduction gas that is utilized strongly impact the way that DRIFTS experiments must be conducted to explore the water gas shift mechanism. For catalysts reduced with CO, researchers in the past have assumed that carbonate decomposition with water addition was evidence for a ceria redox mechanism. However, this is not the case since water addition only activates bridging OH groups by reaction of water with ceria vacancies (and CO_2 removal in the case of residual surface carbonate decomposition). Subsequent CO addition reacts with bridging OH groups to produce surface formates, which are in turn decomposed to CO_2 and H_2 with water addition. The formate mechanism is also strongly suggested by previous isotope switching experiments.

Acknowledgment

The work was supported by the Commonwealth of Kentucky.

References

[1] Fuel Cell Handbook 5th ed., US DOE, NETL (2000).
[2] Fuel Cells for Transportation Program Contractors' Annual Progress Report, US DOE, OAAT (1998).
[3] D.C. Dayton, M. Ratcliff and R. Bain, Fuel Cell Integration-A Study of the Impact of Gas Quality and Impurities, NREL/MP-510-30298 (2001).
[4] A.F. Ghenciu, Curr. Opin. Solid State Mater. Sci. 6 (2002) 389–399.
[5] T. Bunleisin, R. Gorte and G. Graham, Appl. Catal. B 15 (1998) 107.
[6] S. Hilaire, X. Wang, T. Luo, R.J. Gorte and J. Wagner, Appl. Catal. 215 (2001) 271.
[7] Y. Li, Q. Fu and M. Flytzani-Stephanopoulos, Appl. Catal. B 27 (2000) 179.
[8] Q. Fu, A. Weber and M. Flytzani-Stephanopoulos, Catal. Lett. 77(1–3) (2001) 87.
[9] T. Shido and Y. Iwasawa, J. Catal. 141 (1993) 71.
[10] T. Shido and Y. Iwasawa, J. Catal. 136 (1992) 493.
[11] J.C. Lavalley, Catal. Today 27 (1996) 377.
[12] T. Shido and Y. Iwasawa, J. Catal. 129 (1991) 343.
[13] T. Shido, K. Asakura and Y. Iwasawa, J. Catal. 122 (1990) 55.
[14] K. Yamashita, S. Naito and K. Tamaru, J. Catal. 94 (1985) 353.
[15] G. Jacobs, L. Williams, U. Graham, D. Sparks and B.H. Davis, J. Phys. Chem. B, 107 (2003) 10398.
[16] G. Jacobs, L. Williams, U. Graham, G. Thomas, D. Sparks and B.H. Davis, Appl. Catal. A, 252 (2003) 107.
[17] G. Jacobs, P.M. Patterson, L. Williams, E. Chenu, D. Sparks, G. Thomas and B.H. Davis, Appl. Catal. A: Gen., in press.
[18] G. Jacobs, L. Williams, D. Sparks and B.H. Davis, Proc. of the 18th NAM, (Cancun, Mexico, June 2003).
[19] G. Jacobs, S. Khalid, P.M. Patterson, L. Williams, D. Sparks and B.H. Davis, Appl. Catal. A: Gen., in press.
[20] G. Jacobs, P.M. Patterson, U.M. Graham, D.E. Sparks and B.H. Davis, Appl. Catal. A: Gen., in press.
[21] Y. Amenomiya, I.T. Ali Emesh, K.W. Oliver, G. Pleizier, in *Proc. of the 9th ICC (C1 Chemistry)*, Vol. 2, eds. M.J. Phillips and M. Ternan (Chemical Institute of Canada, Ottawa, Ontario, Canada, 1988) p. 634.
[22] X. Montagne, J. Lynch, E. Freund, J. Lamotte, A.J.C. Lavalley, J. Chem. Soc., Faraday Trans. I, 83 (1989) 1451.
[23] A. Laachir, V. Perrichon, A. Badri, J. Lamotte, E. Catherine, J.C. Lavalley, J. El Fallah, L. Hilaire, F. LeNormande, E. Quemere, N.S. Sauvion and O. Touret, J. Chem. Soc. Faraday Trans., 87 (1991) 1601.
[24] R.P. Eischens, W.A. Pliskin and M.J.D. Low, J. Catal., 1 (1962) 180.

[25] C.C. Chang, L.T. Dixon and R.J. Kokes, J. Phys. Chem., 77 (1973) 2634.
[26] C.C. Chang and R.J. Kokes, J. Am. Chem. Soc., 93(1971)7107.
[27] R.J. Kokes, Accounts Chem. Res., 6 (1973) 226.
[28] R.J. Kokes, A.L. Dent, C.C. Chang and L.T. Dixon, J. Am. Chem. Soc., 94 (1972) 4429.
[29] M.F.L. Johnson and J. Mooi, J. Catal. 103 (1987) 502; 140 (1993) 612.
[30] A. Trovarelli, Catal. Rev.- Eng. Sci. 38 (1996) 439.
[31] A. Trovarelli, ed. *Catalysis by Ceria and Related Materials*, Imperial College Press, London, 2002.
[32] S. Bernaal, J.J. Calvino, J.M. Gaatica, J.A.P. Omeil and J.M. Pintado, J. Chem. Soc., Faraday Trans. 89 (1993) 3499.
[33] Lj. Kundakovic, D.R. Mullins and S.H. Overbury, Surf. Sci. 457, 51 (2000).
[34] K. Otsuka, M. Hatano and A. Morikawa, J. Catal. 79 (1983) 493.
[35] J. El Fallah, S. Boujana, H. Dexpert, A. Kiennemann, J. Majerus, O. Touret, F. Villain and F. Le Normand, J. Phys. Chem, 98 (1994) 5522.
[36] J.L.G. Fierro, J. Soria, J. Sanz and J.M. Rojo, J. Solid State Chem, 66 (1987) 154.
[37] S. Bernal, J.J. Calvino, G.A. Cifredo, J.M. Gatica, J.A.P. Omeil and J.M. Pintado, J. Chem. Soc. Faraday Trans. 89 (1993) 3499.
[38] F. Sadi, D. Duprez, F. Gérard and A. Miloudi, J. Catal., 213 (2003) 226.